Bull Soc Chim Fr (1995) 132, 215-223

Stereostructure of glycosylated polyene macrolides : the example of pimaricin

Jean-Marc Lancelin, Jean-Marie Beau*

Université d'Orléans, Laboratoire de Biochimie Structurale associé au CNRS, BP 6759, 45067 Orléans Cedex 2, France

(received 4 July 1994, accepted 30 January 1995)

Summary – On the basis of 2D NMR-derived J coupling constants and qualitative NOEs (ROEs), the 7*S*, 9*R*, 11*S*, 12*R*, 13*S*, 15*R*, 25*R* and 1′*R* configurations of the polyene macrolide pimaricin have been assigned using the sugar D-mycosamine as an internal chiral reference. Perhydrogenation of the carbon-carbon double bonds and simultaneous regiospecific hydrogenolysis of the epoxide function on *N*-acetyl pimaricin furnished a single 5,7-diol system. Acid-catalyzed bicycloketalization led to two spiroketals in which the configuration at C_5 was found to be *R*, thus defining the remaining 4*R* and 5*R* chiral centers of pimaricin.

polyene macrolide / pimaricin / stereostructure / NMR spectroscopy

Introduction

Pimaricin (also known as natamycin or myprozine), a representative glycosylated polyene macrolide [2], was first isolated in 1957 from *Streptomyces natalensis* [3]. Another antifungal antibiotic, tennecetin, produced by *S chattanoogensis* [4], was later shown to be identical to pimaricin [5]. Its correct covalent structure was finally established [6] as **1** after a number of erroneous proposals [7, 8], indicative of the difficulties encountered in the structural determination of these types of substances.

The clinical value of polyene macrolide antibiotics lies mainly in their antifungal activity. Other significant biological properties of some of these substances [9], such as their ability to stimulate the immune response at lower concentrations [10] and their action in synergy with other antifungal compounds [11, 12] or antitumor drugs [13, 14], have incited recent interest in their stereochemical assignment [15]. Precise knowledge of their stereostructure is of primary importance for conformational analysis in relation to biological activity, and for conducting any predictive chemical modifications or total synthesis.

Past spectroscopic investigations have revealed the following characteristics for the macrocycle : a) the *E* geometry of the C_2-C_3 double bond by ^1H NMR studies [16]; b) the *trans*-epoxide moiety at C_4-C_5 [18]; c) a hemiacetal function at C_9 confirmed by ^{13}C NMR [17, 18] and CD [18] spectra, and the chair conformation of the C_9-C_{13} cyclic segment with the substituents in equatorial positions [16]; and d) the all-*E* C_{16}-C_{23} tetraene segment [19].

The D-series of the mycosamine was established by mixed-melting point X-ray powder diffraction considerations [7a] and the β-glycosidic linkage proposed was based on the $J_{C1'-H1'}$ coupling constant value [16a]. Although an X-ray investigation of pimaricin crystals was reported in 1977 [20], no tridimensional structure could be deduced from these data.

More recently, a controlled degradation protocol designed for stereostructural studies was developed by Fraser-Reid for this antibiotic leading to a C_3-C_{16} segment, a possible target for synthetic work [21]. Here we give a detailed account of our preliminary report [22], which defined the complete stereostructure of pimaricin. Shortly after our communication, Duplantier and Masamune [23] reported studies based on the reagent-controlled asymmetric synthesis of diastereoisomers which also defined the stereochemistry of pimarolide thus representing the first synthetic access to this macrocycle.

Results and discussion

NMR spectroscopy of pimaricin **1** *and* N*-acetyl pimaricin* **2**

We have previously shown for nystatin A1 [24] that the combined use of double quantum filtered COSY (DQF-COSY) [25], rotating frame Overhauser spectroscopy (ROESY) [26, 27] and NOESY [28, 29] allowed the determination of the relative configurational features of the macrolide. The configurations were converted from relative to absolute by seeking unambiguous proton-proton through-space contacts with the sugar D-mycosamine taken as an internal chiral probe. This strategy has also been used successfully by Sowinski *et al* [30] to determine the stereostructure of vacidin A, another macrolide of the heptaene family. For pimaricin,

* Correspondence and reprints

Table I. 300 MHz ^{1}H NMR data from phase sensitive DQF-COSY of pimaricin **1** (10 mM in MeOH-d_4, 298°K, residual CD_3OH as internal reference = 4.82 ppm) and *N*-acetyl pimaricin **2** (15 mM in DMSO-d_6, 303°K, residual DMSO as internal reference = 2.49 ppm).

	Pimaricin **1**		*N*-Acetyl pimaricin **2**	
Proton	δ (ppm)	Coupling partner[a] (J, Hz)[b]	δ (ppm)	Coupling partner (J, Hz)[b]
2	6.02	H3 (15.8) H4 (0.6)	6.11	H3 (15.6)
3	6.38	H4 (7.5)	6.25	H4 (7.5)
4	3.12	H5 (1.5)	3.22	H5 (2.5)
5	2.79	H6ax (1.8) H6eq (8.3)	2.73	H6ax (0-1) H6eq (8.1)
6ax[c]	2.00	H6eq (−14.4) H7 (0∼1)	1.93	H6eq (−17.6) H7 (0∼1)
6eq[c]	1.16	H7 (11)	1.14	H7 (10.3)
7	4.28	H8ax (0-2) H8eq (10.2)	4.11	7OH (5) 8ax (0∼1) H8eq (8)
7OH	–	–	5.30	–
8ax	1.55	H8eq (−14.2)	1.50	H8eq (−13.8)
8eq	1.66	–	1.58	–
9OH	–	–	6.15	H10ax (0.5∼1)
10ax	1.23	H10eq (−12.4) H11 (11)	1.12	H10eq (−13.8) H11 (10.8)
10eq	1.95	H11 (4.8)	1.83	H11 (4.5)
11	4.25	H12 (10.5)	4.00	H12 (9.6)
12	1.95	H13 (10.5)	1.93	H13 (10.8)
13	4.34	H14ax (8.4) H14eq (0∼2)	4.19	H14ax (8.8) H14eq (0.1)
14ax[c]	1.57	H14eq (−14) H15 (2)	1.57	H14eq (−15.1) H15 (3)
14eq[c]	2.28	H15 (3.5)	1.96	H15 (5)
15	4.38	H16 (8.3)	4.37	H16 (8.8)
16	5.95	H17 (15.3)	5.84	H17 (15.5)
17	6.11	H18 (10)	6.09	H18 (10.6)
18	6.43	–	6.48	H19 (16.6)
19	6.18	–	6.21	H20 (10.1)
20	6.15	–	–	–
21	6.15	–	–	H22 (10.1)
22	6.10	H23 (15.4)	6.04	H23 (14.6)
23	5.56	H24ax (8.8) H24eq (2.5)	5.59	H24ax (10.1) H24eq (5)
24ax[c]	2.20	H24eq (−13.5) H25 (11)	2.18	H24eq (−13.5) H25 (11.5)
24eq[c]	2.36	H25 (5.6)	2.38	H25 (2.5)
25	4.68	$26CH_3$ (6.5)	4.67	$26CH_3$ (6.5)
$26CH_3$	1.28	–	1.23	–
1′	4.53	H2′ (1)	4.35	H2′ (1)
2′	3.98	H3′ (3.5)	3.52	2′OH (6.5) H3′ (3)
2′OH	–	–	4.54	–
3′	3.16	H4′ (9)	3.65	NH (8.3) H4′ (9.5)
NH	–	–	7.59	–
4′	3.35	H5′ (9)	3.10	4′OH (5.5) H5′ (9.5)
4′OH	–	–	4.63	–
5′	3.28	$6'CH_3$ (6.5)	3.14	$6'CH_3$ (6.5)
$6'CH_3$	1.24	–	1.14	–
$COCH_3$	–	–	1.84	–

[a] The coupling partner is listed only once according to the proton having the lower number. [b] The J coupling constants are measured at ±0.2 Hz on a 1D resolution enhanced spectrum. Two values are indicated when the coupling constants were estimated directly from the splitting of the 2D DQF-COSY spectrum. [c] Refers to the pseudo-axial (ax) or pseudo-equatorial (eq) orientation of these protons relative to the average plane of the macrocycle.

we first established the D-series of mycosamine by a standard deglycosylation in MeOH under acidic conditions, followed by acetylation to the di-*O*-acetate **4** (fig 1) identical to an authentic sample obtained from nystatin A1 [31].

The saturation of pimaricin **1** in MeOH-d_4 at room temperature led to an approximately 10 mM solution, suitable for NMR studies on a medium-field strength spectrometer. Higher concentrations were easily obtained in DMSO-d_6, where the natural line-width of the proton resonances increased by 2-3 Hz at concentrations similar to those used with MeOH-d_4 (increased viscosity). Assignments of the proton resonances for the macrocycle as well as for the mycosamine appendage were obtained from DQF-COSY alone. Figure 2 shows a representative part of the DQF-COSY used for the assignment. The three independent uninterrupted coupled proton spin systems corresponding to the C_2-C_8 and C_{10}-C_{25} segments and the mycosamine moiety in **1** were identified and specifically assigned. The J coupling constants were measured on either the DQF-COSY spectra or resolution-enhanced 1D spectra for all protons in MeOH with the exception of the C_{18} to C_{21} segment because of a chemical shift degeneration of the proton resonances. The J coupling constants for this portion of the molecule were obtained in DMSO-d_6, a solvent in which the resonances were better separated on **1** and the *N*-acetyl derivative **2**. Four additional and

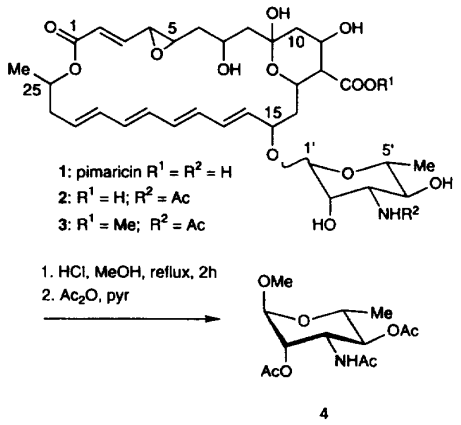

Fig 1. Deglycosylation of pimaricin **1**.

exchangeable resonances were further observed for **2** in this situation. They were readily assigned by DQF-COSY to the respective hydroxyl protons at positions C_7 and C_9 of the macrocycle, and $C_{2'}$ and $C_{4'}$ of the *N*-acetyl-D-mycosamide moiety. Neutralization of the amino group by the formation of **2** decreased the exchange rates of hydroxyl protons which were observed as a unique broad resonance (*ie*, in fast exchange rates on the NMR time-scale) at δ 4.25 ppm for pimaricin **1** in DMSO. The remaining hydroxyl proton at C_{11}, β to the carboxyl group, was further observed for only the methyl ester **3** of **2**. The different proton chemical shifts and *J* coupling constant assignments for pimaricin **1** and its *N*-acetyl derivative **2** are summarized in table I.

At this stage several structural assignments could be deduced from the scalar couplings. First, the chair conformation of the C_9-C_{13} fragment with the substituents all equatorial at C_{11}, C_{12} and C_{13} (J_{10a-11} = 11.0, $J_{10e,11}$ = 4.8, $J_{11,12}$ = 10.5 and $J_{12,13}$ = 10.5 Hz) confirmed the previous observations [16-18]. In addition, the axial orientation of the OH_9 in **2** could be assigned by the long-range coupling constant with H_{10a} ($J_{OH9-H10a}$ = 0.5-1 Hz) requiring a conformation in which the four bonds H_{10a}-C_{10}-C_9-O_9-H_9 are nearly coplanar (W-arrangement [33]). Such long-range coupling constants had already been observed for the hydroxyl groups in a nystatin A1 fragment [32], but was observed here for the first time in a native polyene macrolide structure.

The different proton spin systems identified in the DQF-COSY spectra were connected by ROESY and NOESY experiments. In MeOH, the NOEs observed were positive effects leading to NOESY off-diagonal connectivities in antiphase relative to the diagonal, in accordance with the motional regime of small molecules in an organic solvent that fulfills the condition $\tau_c < 1.12\omega_0^{-1}$ [34]. Conversely, in DMSO neither pimaricin **1** nor its *N*-acetyl derivative **2** exhibited connectivities at 25°C ($\tau_c \cong 0.5$ ns) and the dipolar connectivities were extracted from only ROESY experiments. Table II and figure 3 describe the NOE connectivities observed in ROESY and/or NOESY experiments for pimaricin **1** and the *N*-acetyl derivative **2**. Using these dipolar couplings, several new structural assignments could be made. First, the NOE connectivities between H_8 and H_{10} protons define the diastereotopicity of the H_8 protons (intensities of the NOE contacts between the *anti* protons, *eg*, H_{8ax}-H_{10eq} and H_{8eq}-H_{10ax} were systematically weaker than those of the *syn* protons, H_{8ax}-H_{10ax} and H_{8eq}-H_{10eq}; see table II), hence the configuration at C_7 relative to the C_9-C_{13} tetrahydropyran ring ($J_{8a,7}$ = 0-2, $J_{8e,7}$ = 10.2 Hz). Next, an accurate local geometry of the C_{13}-C_{16} segment was deduced from a set of well-defined coupling constants ($J_{13,14a}$ = 8.4, $J_{13,14e}$ = 1.0, $J_{14a,15}$ = 2.0, $J_{14e,15}$ = 3.5, and $J_{15,16}$ = 8.3 Hz) and from the NOEs between the proton pairs H_{13}-H_{16} and H_{15}-H_{17}. These observations

Table II. NOEs (ROEs) observed from NOESY (ROESY) experiments of pimaricin **1** (10 mM in MeOH-d_4, 298°K) and *N*-acetyl pimaricin **2** (15 mM in DMSO-d_6, 303°K)[a,b].

Proton	Pimaricin **1**	*N*-Acetyl pimaricin **2**[c]
2	H4	H4
3	H5	H5
4	H6eq, H6ax[e]	H6eq, H6ax[e]
5	H7	H7, 7OH, H18
6ax[d]	H8ax, H8eq[e]	–
6eq[d]	H8eq, H8ax[e]	7OH
7	H18	H16, H17, 9OH
7OH	–	9OH, H18
8ax	H10ax, H10eq[e]	–
8eq	H10eq, H10ax[e]	–
9OH	–	H13
10ax	–	–
10eq	–	–
11	–	H13
12	H14ax	–
13	H2′, H16	H16
14ax[d]	–	–
14eq[d]	H1′	H1′
15	H17, H1′	H17
16	H18	H18
17	–	–
18	–	–
19	–	–
20	–	–
21	–	–
22	H24ax	–
23	H25	H25
24ax[d]	$26CH_3$	$26CH_3$
24eq[d]	$26CH_3$	$26CH_3$
25	–	–
$26CH_3$	–	–
1′	H3′, H5′	H3′, H5′
2′	–	–
2′OH	–	–
3′	–	–
3′NH	–	–
4′	$6'CH_3$	$6'CH_3$
4′OH	–	–
5′	–	–
$6'CH_3$	–	–

[a] Contacts between scalar coupled protons are not cited. ROEs (NOEs) are listed only once according to the proton having the lower number. [b] Positive effects in both NOESY and ROESY experiments. [c] No NOEs were observed under the conditions used (300 MHz, DMSO-d_6, 303°K). [d] Refers to the pseudo-axial (ax) or pseudo-equatorial (eq) orientation of the protons relative to the average plane of the macrocycle. [e] Contacts of weaker intensities.

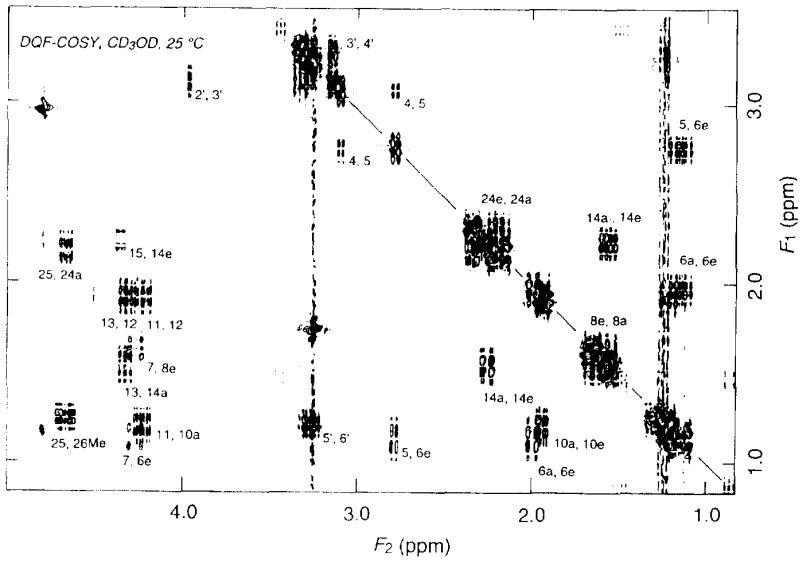

Fig 2. Plot of the aliphatic (F_2, F_1) region of the DQF-COSY spectrum of pimaricin **1**, recorded at 25°C (10 mM in CD_3OD). Positive and negative contours are distinguished with open and filled contours, respectively. The diagonal is drawn as a line. The F_1 noise strips at δ 3.25 and 1.25 pm are due to the residual CD_2H signal of the solvent and the 26-6′ CH_3 signals of pimaricin, respectively.

define the diastereotopicity of the H_{14} protons (see fig 3) and thus the configuration at C_{15} relative to that at C_{13}.

Once the C_7 to C_{15} relative stereostructure was defined, we focused our attention on the through-space contacts between the D-mycosamine and the macrocycle protons. The β-configuration of the anomeric linkage at O_{15} was first established through the NOEs between $H_{1'}$-$H_{5'}$ and $H_{3'}$-$H_{5'}$, which confirms the previous suggestion [16]. The proximity of the anomeric proton $H_{1'}$ to both H_{14e} and H_{15} of the aglycon could then be deduced from the NOE observed between these positions. A third NOE between $H_{2'}$ (sugar) and H_{13} (macrocycle) was observed under various conditions. Only an *R* configuration at C_{15} conformed to these last three NOE distance constraints. Figure 4 shows the representative part of a ROESY experiment where these key effects were observed. Aside from our own studies on nystatin A1 [24], these pivotal NOE effects were recently detected in two other polyenes, the heptaenes vacidin A [30] and candidin [35], and amphotericin B [36], the only polyene glycosylated by mycosamine for which a crystallographic structure has been reported [37]. Consequently, the 7*S*, 9*R*, 11*S*. 12*R*, 13*S*, and 15*R* were assigned for the pimaricin aglycon [38].

The isolated C_{25} stereocenter

The difficult task of defining the absolute configuration of the isolated C_{25} stereocenter turned out to be rather simple. Taking the combined data from the DQF-COSY map ($J_{23,24a}$ = 8.8, $J_{23,24e}$ = 2.5, $J_{24a,25}$ = 11.0 and $J_{24e,25}$ = 5.6 Hz, table I) easily provided a precise local geometry for the C_{22}-C_{25} portion of the molecule. The best resolution for the olefinic protons of the C_{16}-C_{23} tetraene segment was exhibited by the DQF-COSY spectrum of the *N*-acetyl pimaricin **2**. Only the $J_{20,21}$ coupling constants remained undetermined [19]. The ^3J values of 10.1 to 10.6 Hz for the H_{17}-H_{18}, H_{19}-H_{20} and H_{21}-H_{22} pairs (all protons antiperiplanar by pairs) showed an all-*E* *extended* conformation of the tetraene. This important observation permitted transmission of the stereostructural information from H_{16} to H_{23}, the two ends of the molecular rod, and hence the orientation of the C_{23}-C_{25} segment relative to the C_9-C_{16} segment was defined. This information, combined with the C_{23}-C_{25} local geometry described above, defined the diastereotopicity of the H_{24} protons (see fig 3) and, as a consequence, the *R* configuration at C_{25}.

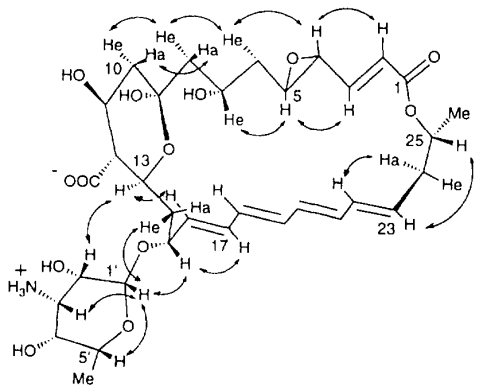

Fig 3. Diagnostic ROEs observed on pimaricin **1** and shown as bidirectional arrows.

The C_4-C_5 epoxide function

The spectroscopic study above provided ambiguous stereochemical information on the epoxide function due to the quasi-planar arrangement of H_4-C_4-C_5-H_5. Regioselective opening of the epoxide function by hydrides

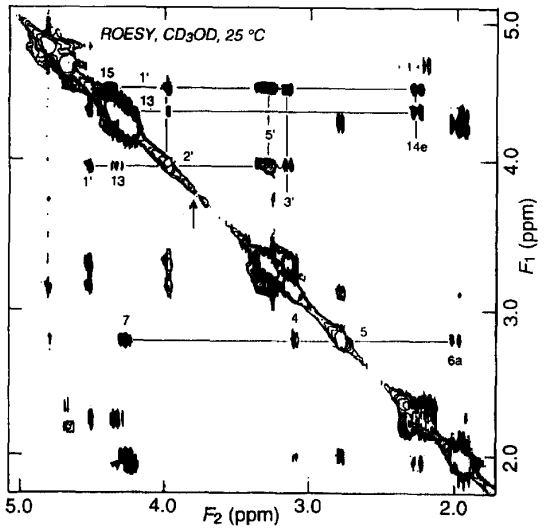

Fig 4. Part of the ROESY spectrum of pimaricin **1**, (250 ms mixing time) recorded at 25°C (10 mM in CD_3OD). Positive and negative contours are distinguished as open and filled areas, respectively. Assignments of ROEs for $H_{1'}$, $H_{2'}$ and H_5 are shown along the F_2 dimension. The arrow indicates the carrier frequency position upon which the Hartman-Hahn transfer (positive contours) between $H_{2'}$, $H_{3'}$, $H_{4'}$ and $H_{5'}$ is strongly dependent [27].

at the allylic carbon C_4 would have furnished a 1,3-diol at C_5-C_7, a hydroxylation pattern found in tetrin A, tetramycin A or arenomycin B [2b] readily amenable to spectroscopic analysis. This single operation was not productive on **2**, **3** or the corresponding persilylated derivatives [21], since no reagents could be found that would not affect the polyene segment of the molecule. Treatment of **3** with methanethiol in MeOH-Et_3N, conditions known to affect vinylic epoxides, led, however, to a single compound **5**, resulting from a conjugate addition to the α,β-unsaturated lactone (fig 5). The structure was established by an analysis of the DQF-COSY in MeOH-d_4 where the typical olefinic AB spin system of pimaricin at C_2-C_3 (δ 6.02, 6.38) was replaced by an ABX spin system at δ 2.47, 2.57, and 2.77 respectively, representative of methylene protons β to a carbonyl group and coupled to a proton of a sulfur-substituted methine group. Unfortunately, the J coupling pattern of the new C_2-C_4 structural segment ($J_{2A,3}$ = 8.5, $J_{2B,3}$ = 5.0, and $J_{3,4}$ = 8.5 Hz) did not allow a straightforward, unambiguous assignment of the configuration at C_3. Although this clean transformation with diols is of no use for our purpose, it may represent a useful process for an easy modification of the natural antibiotic.

At this stage is was most probable that breaking up the structural rigidity of the macrolactone combined with a regioselective epoxide opening would lead to a conformationally biased bicycloketal in which the configuration at C_4 (or C_5) could easily be assessed. Hydrogenolysis and methyl ester formation on *N*-acetylpimaricin **2** provided a single saturated polyol **6** (fig 6). A ^1H NMR spectrum on **6** obtained in DMSO-d_6 showed all hydroxyl resonances at δ 4.48 ($OH_{2'}$, J 5.0 Hz), 4.54 (OH_5, J 5.0 Hz), 4.60 (OH_4, J 5.9 Hz),

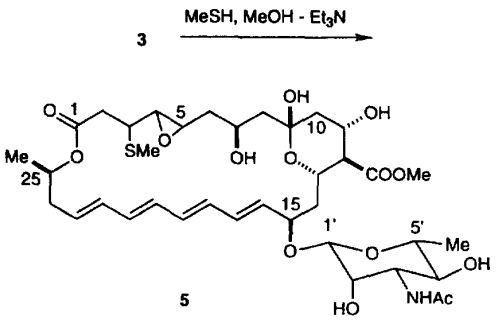

Fig 5. Methanethiol treatment of *N*-acetyl pimaricin methyl ester **3**.

4.88 (OH_{11}, J 6.3 Hz), 4.92 (OH_7, J 5.8 Hz) and 5.92 (OH_9, $J \sim 1$ Hz) (table III). It was easy to deduce that a hydroxyl group was located at C_5 from the phase-sensitive DQF-COSY spectrum which revealed the 5,7-diol pattern with H_5 (3.60 ppm), two H_6 (1.39-1.49 ppm) and H_7 (4.08 ppm) (table III). A similar transformation on **2** was described by Ceder *et al* [16a] to give a hydroxyl group at C_4 in contradiction to the previous findings of Golding *et al* [6]. This transformation placed the hydroxyl group at C_5 as a result of the allylic hydrogenolysis of the epoxide moiety for which, unfortunately, no precise experimental conditions were given [39]. Our results are in full agreement with Golding's conclusions.

Acidic treatment of **6** (CSA cat $CHCl_3$/MeOH, 9:1) for 2 h at room temperature gave the two easily separated bicycloketals **7** and **8** (80%) in a 1.2 to 1 ratio, respectively. At this point, the important 1971 report of Rinehart *et al* [40] should be mentioned. In a structural investigation on tetrin A, these authors reported, for comparison, a sequence of transformations on pimaricin which included : a) hydrogenation over platinum oxide in glacial acetic acid; b) peracetylation; and c) esterification with diazomethane in ethyl ether. They obtained «a methyl ester of pentaacetyldecahydropimaricin rather than the expected heptaacetyl derivative» about which they stated that «possible explanations are hydrogen bonding and steric hindrance». It is most probable that a compound identical to **7** or **8** was obtained by bicycloketalization in the course of the acidic hydrogenation step. The same conclusions should be considered for the work on tetrin A [40] and tetrin B [41]. A ratio of 40:1 (85% yield) was obtained when the same acidic treatment of **6** was prolonged for 72 h. This behavior strongly suggests a 5,7-*syn*-diol pattern as depicted in figure 7.

A rough estimate of the stabilizing electronic effects [42] and the destabilizing $A_{1,3}$ effects when the two isomers are placed under equilibrating acidic conditions showed that **A1/A2** would equilibrate in a ratio of approximately 1:1 (no differences were observed between the two isomers) whereas **S1/S2** would give an equilibrium much in favor of **S1**. This prediction was fully confirmed by ^1H NMR analysis of the tetra-*O*-acetate **9** (major isomer) and **10** (minor isomer) (tables III and IV). The coupling constants observed led to chair-chair bicycloketals with a splitting pattern only consistent

Table III. 300 MHz ^{1}H NMR data from phase-sensitive DQF-COSY of **6** (15 mM in DMSO-d_6, 298°K, residual DMSO as internal reference = 2.49 ppm) **9** and **10** (20 mM in C_6D_6, 300°K, residual C_6H_6 as internal reference = 7.16 ppm).

Proton	**6** δ (ppm)	**6** Coupling partner[a] (J, Hz)[b]	**9** δ (ppm)	**9** Coupling partner (J, Hz)[b]	**10** δ (ppm)	**10** Coupling partner (J, Hz)[b]
5	3.60		3.94	H4,4″ (6.0) H6ax (11.5) H6eq (1.9)	3.77	H6ax (8.9) H6eq (3)
5OH	4.54	H_5 (5.0)	–	–	–	–
6ax[c]	1.39-1.49	–	1.19	H6eq (−15) H7 (3.1)	1.49	H6eq (−13.7) H7 (3.9)
6eq[c]			1.55	H7 (4.5) H8eq (1∼2)	1.59	H7 (4.8) H8eq (5.5) H8ax (4.5)
7	4.08		4.99	H8ax (4) H8eq (3.3)	5.17	–
7OH	4.92	H7 (5.8)	–	–	–	–
8ax[c]	1.60	–	1.23	H8eq (−15)	1.80[d]	H8eq (−14.3)
8eq[c]		–	1.98	–	1.97[d]	–
9OH	5.92	H10ax (0∼2)	–	–	–	–
10ax	1.18	H10eq (−13.5) H11 (10.5)	1.27	H10eq (−12.8) H11 (10.9)	1.57	H10eq (−12) H11 (10.9)
10eq	1.97	H11 (4.5)	2.11	H11 (4.9)	2.88	H11 (4.7)
11	4.01	11OH (6.3) H12 (10.5)	5.86	H12 (10.9)	5.50	H12 (10.9)
11OH	4.88	–	–	–	–	–
12	2.05	H13 (10.5)	2.57	H13 (10)	2.76	H13 (9.6)
13	3.98	H14 (9) H14″ (1-2)	4.17	H14 (10.3) H14″ (1.5)	4.04	H14 (8.6) H14″ (3.5)
14	1.64	H14″ (−13.5) H15 (2∼3)	2.03	H14″ (−13.7) H15 (3.1)	1.99	H14″ (−14.2) H15 (3.5)
14″	1.41	H15 (7.5)	1.76	H15 (10.4)	1.79	H15 (7.7)
15	3.74	–	4.17	–	4.05	–
25	4.81	26CH_3 (6.5)	5.12	–	5.10	–
26CH_3	1.13	–	1.07	H25 (6.5)	1.09	H25 (6.5)
COOCH_3	3.61	–	3.36	–	3.49	–
1′	4.30	H2′ (1)	4.44	H2′ (1)	4.51	H2′ (1)
2′	3.49	2′OH (5.0) H3′ (3.5)	5.59	H3′ (3.5)	5.65	H3′ (3.5)
2′OH	4.48	–	–	–	–	–
3′	3.63	3′NH (8.2) H4′ (9.5)	4.54	3′NH (8.9) H4′ (9.5)	4.56	3′NH (8.9) H4′ (9.5)
3′NH	7.60	–	5.51	–	5.62	–
4′	3.11	4′OH (5.9) H5 (9.5)	5.00	H5′ (10.5)	5.02	H5′ (10.5)
4′OH	4.60	–	–	–	–	–
5′	3.13	6′CH_3 (6.5)	3.20	6′CH_3 (6.5)	3.27	6′CH_3 (6.5)
6′CH_3	1.13	–	1.10	–	1.22	–
NHCOCH_3	1.83		2.04	–	2.00	–
OCOCH_3	–		1.84	–	1.88	–
			1.68		1.65	–
			1.65	–	1.64	–
			1.59	–	1.55	–

[a] The coupling partner is listed only once according to the proton having the lower number. [b] See *b*, table I. [c] For **6**, this refers to the pseudo-axial (ax) or pseudo-equatorial (ex) orientation of these protons relative to the average plane of the macrocycle. [d] Assignments by NOE experiments.

with an equatorially disposed H_7 (all coupling constant values less than 5.5 Hz) in both isomers.

These conformational and configurational features were validated by the intracyclic NOE (ROE) contacts H_{10ax}-H_{12} and H_{11}-H_{13} in both **9** and **10** (table IV). Further, these rigid bicyclic systems exhibited long-range space contacts (H_5-H_{13} in **9** and H_5-H_{10eq}, H_{8eq}-H_{11} in **10**), an observation that allowed the assignment of the absolute configuration at the spiro center in **9** and **10** as shown in figures 6 and 7. The *R* configuration at C_5 of the natural antibiotic was thus deduced and by correlation, the *R* configuration at C_4. The complete stereostructure of pimaricin as **11** was hence defined (fig 8).

Experimental section

General methods

TLC was performed on silica gel (Merck F-254 plates) in the specified solvent systems. Chromatographic separations were carried out on silica (Merck 60, 0.2-0.063 mm). Optical rotations were determined on a Perkin Elmer polarimeter, Model 141. Combustion analyses as well as MS spectra were done at the Service Central d'Analyses (CNRS, Vernaison, France). Molecular formula were checked by FABMS at 2000 resolution on selected pseudo-molecular ions and their isotopic clusters by multichannel analysis (MCA) leading to a resolution of 0.06 atomic mass unit or by liquid secondary ion mass spectrometry (LSIMS) with a Fisons-VG type ZAB2.SEA spectrometer.

NMR spectroscopy

Samples were dissolved in 0.5 mL of the specified highest-available NMR grade deuteriated solvent (Aldrich) and thoroughly degased by the freeze-thaw technique and sealed under vacuum in a 5 mm diameter tube (Wilmad). Spectra were recorded at 25°C for samples in methanol, and 30 or 40°C for samples in DMSO, on a Bruker AM spectrometer operating at 300 MHz for the proton frequency. ^{1}H 2D

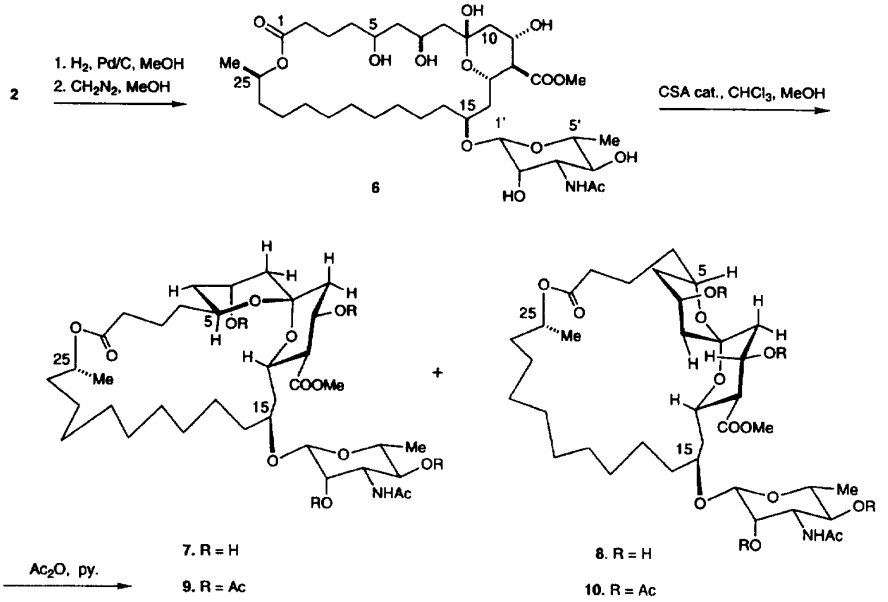

Fig 6. Formation of spiroketals **9** and **10** from *N*-acetyl pimaricin **2**.

Table IV. NOEs (ROEs) observed from NOESY (ROESY) experiments on **9** (major isomer) and **10** (minor isomer) in C_6D_6 at 300°K[a,b].

Proton	9	10
5	H13	H10eq
6ax	–	–
6eq	–	–
7	–	–
8ax	–	H11[c]
8eq	–	H11[c], H13[d]
10ax	H12	H12
10eq	–	–
11	H13	H13
12	–	–
13	–	–
14	H1′	–
14″	–	–
15	H1′	H1′
1′	H3′, H5′	H3′, H5′
2′	–	–
3′	H5′	H5′
3′NH	H4′	H4′
4′	6′CH_3	6′CH_3
5′	–	–
6′CH_3	–	–

[a] Positive effects at 300°K. [b] Contacts between the scalar coupled protons are not listed. ROEs (NOEs) are listed only once according to the proton having the lower number. [c] The H8eq-H11 interaction stronger than the H8ax-H11 interaction. [d] Overlaped with the H13-H14 connectivity.

spectra, DQF-COSY (double quantum filtered correlation spectroscopy) [25], ROESY (rotating frame Overhauser effect spectroscopy) [26, 27], and NOESY (nuclear Overhauser spectroscopy) [28, 29] spectra were recorded in the phase-sensitive mode using the TPPI (time phase proportional increment) method [43]. Two-dimensional spectra were collected as 256 (t_1) and 4 096 (t_2) complex point time-domain matrix with a spectral width of 1 800 Hz in both dimensions

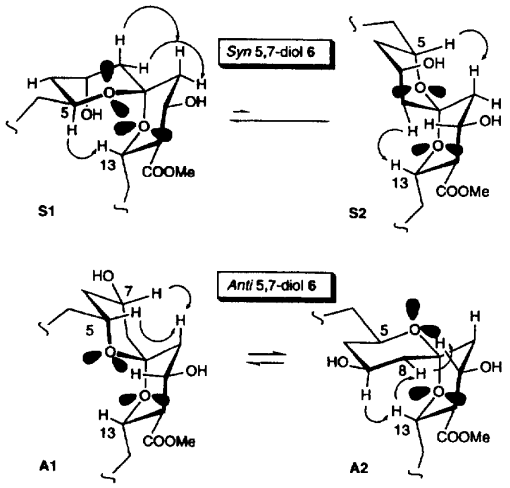

Fig 7. Chair-chair spiroketals formed from the possible *syn*-diol **6** (**S1,S2**) or the *anti*-5,7-diol **6** (**A1,A2**). The arrows indicate the NOEs observed for **S1,S2** and the close contacts that would give detectable NOEs for **A1,A2**.

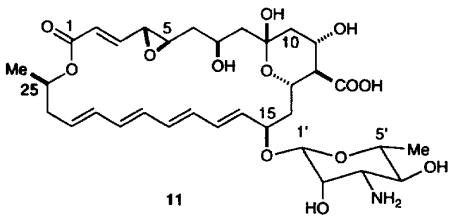

Fig 8. Complete stereostructure of pimaricin **1**.

and 16 scans per t_1 increments. They were transformed after zero-filling in the $F1$ dimension into 512 and 2 048 real

points in $F1$ and $F2$ dimensions using Bruker DISNMR software.

Methyl 3-acetamido-2,5-di-O-acetyl-3,6-dideoxy-α,D-mannopyranoside **4**

To a solution of pimaricin **1** (835 mg, 1.28 mmol) in absolute methanol (25 mL), dry hydrogen chloride was bubbled through for 0.5 h. The mixture was refluxed for 2 h and stirred at room temperature overnight. The solvent was removed under reduced pressure and the dark-green residue was dissolved in water (15 mL) and washed with dichloromethane portions (10 mL) until the organic layer remained colorless. The aqueous layer was then washed twice with *n*-butanol (1 mL), and then evaporated under reduced pressure and dried *in vacuo* to give crude crystalline methyl-D-mycosamine hydrochloride (251 mg). The latter was directly acetylated in pyridine (5 mL) and acetic anhydride (6 mL) to give, after work-up, a pale-yellow syrup which crystallized in ethyl ether (348 mg, 99%). The product was recrystallized from ether/pentane four times until a constant melting point was reached, mp 138-140°C (lit [31], 140°C).

$[\alpha]_D^{23}$ +30 (*c* 0.99, EtOH) {lit [44]; $[\alpha]_D^{23}$ +33 (*c* 1.0, EtOH)}.

^{1}H NMR (300 MHz, $CDCl_3$): δ 1.21 (d, 3H, *J* 6.3 Hz, 6-CH_3), 1.92, 2.07, 2.17 (3s, 3H each, OAc and NHAc), 3.58 (s, 3H, OMe), 3.92 (dq, 1H, $J_{5,4}$ 10.5, $J_{5,6}$ 6.3 Hz, H_5), 4.61 (m, 1H, $J_{3,2}$ 3.3, $J_{3,4}$ 9.8, $J_{3,NH}$ 8.9 Hz, H_3), 4.66 (d, 1H, $J_{1,2}$ 1.6 Hz, H_1), 4.79 (dd, 1H, $J_{4,5}$ 10.5, $J_{4,3}$ 9.8 Hz, H_4), 4.93 (dd, 1H, $J_{2,1}$ 1.6, $J_{2,3}$ 3.3 Hz, H_2), 5.58 (d, 1H, $J_{NH,3}$ 8.9 Hz, NH).

N-*Acetyl pimaricin methyl ester-methanethiol adduct* **5**

To a suspension of *N*-acetyl pimaricin methyl ester **3** (114 mg, 0.16 mmol) in absolute methanol (7 mL) and anhydrous triethylamine (1 mL) cooled at 0°C was added, with the aid of a dry-ice condenser, methanethiol (7 drops). The mixture rapidly became homogeneous and was stirred for 1 h at 0°C and then evaporated *in vacuo* to give a white amorphous powder (125 mg) which was purified on a column (17 g) with chloroform/methanol (87:13, v/v) as eluent giving compound **5** (72 mg, 59%).

$[\alpha]_D^{23}$ +145 (*c* 1.58, MeOH).

^{1}H NMR (25°C, MeOH-d_4): δ 1.11 (m, 1H, *J* 8.5, 9.2, 14.0 Hz, H_{6eq}), 1.25 (dd, 1H, *J* 10.9, 14.0 Hz, H_{10eq}), 1.26 (d, 6H, 6.5 Hz, 6′-CH_3 and 26-CH_3), 1.57 (dd, 1H, *J* 2.0, 14.0 Hz, H_{8eq}), 1.72 (m, 1H, *J* 1.5, 8.5, 14.0 Hz, H_{14ax}), 1.72 (dd, 1H, *J* 10.2, 14.0 Hz, H_{8ax}), 1.96 (m, 1H, *J* 0.5, 2.7, 14.5 Hz, H_{6ax}), 1.98 (s, 3H, NHAc), 1.98 (m, 1H, *J* 2.0, 8.5, 14.0 Hz, H_{14eq}), 2.01 (dd, 1H, *J* 4.5, 14.0 Hz, H_{10eq}), 2.17 (s, 3H, SCH_3), 2.19 (m, 1H, *J* 10.0, 11.0, 13.5 Hz, H_{24ax}), 2.24 (t, 1H, *J* 10.5 Hz, H_{12}), 2.38 (m, 1H, *J* 2.5, 5.6, 13.5 Hz, H_{24eq}), 2.47 (dd, 1H, *J* 8.5, 16.5 Hz, H_{2A}), 2.57 (dd, 1H, *J* 5.0, 16.5 Hz, H_{2B}), 2.77 (m, 1H, *J* 5.0, 8.5 Hz, H_3), 2.85 (m, 2H, $H_{4,5}$), 3.28 (m, 2H, $H_{4',5'}$), 3.55 (dd, 1H, *J* 1.0, 3.0 Hz, $H_{2'}$), 3.82 (dd, 1H, *J* 3.0, 9.5 Hz, $H_{3'}$), 4.21 (m, 1H, *J* 4.5, 9.6, 10.8 Hz, H_{11}), 4.28 (m, 1H, *J* 1.0, 8.0, 10.3 Hz, H_7), 4.35 (m, 1H, *J* 1.5, 7.5, 10.8 Hz, H_{13}), 4.45 (m, 1H, *J* 1.5, 3.5, 8.3 Hz, H_{15}), 4.49 (d, 1H, *J* 1.0 Hz, $H_{1'}$), 4.90 (m, 1H, *J* 2.5, 6.5, 11.5 Hz, H_{25}), 5.58 (m, 1H, *J* 5.0, 10.2, 15.6 Hz, H_{23}), 5.87 (dd, 1H, *J* 10.5, 15.6 Hz, H_{16}), 6.00 ~ 6.25 (m, 5H, $H_{17,19,20,21,22}$), 6.35 (m, 1H, *J* 10.5, 16.5 Hz, H_{18}).

MS (FABMS): *m/z* 809 ($M + K^+$), 793 ($M + Na^+$), 771 ($M + H^+$), 753 ($M + H^+ - H_2O$).

MCA-FABMS calc for $C_{37}H_{55}NO_{14}S$ + Na: 792.3241, found 792.32.

Anal calc for $C_{37}H_{55}NO_{14}S \cdot H_2O$: C, 56.40; H, 7.29. Found: C, 56.40; H, 7.29.

Perhydro-pimaricin methyl ester **6**

A stirred suspension of *N*-acetyl pimaricin **2** (738 mg, 1.04 mmol) in methanol (75 mL) was treated by hydrogen (50 psi) in the presence of 10% palladium on carbon. After 1.5 h, the catalyst was filtered and thoroughly washed with methanol (75 mL). The solution was concentrated up to half the volume (~ 75 mL) under reduced pressure and directly treated with an etheral solution of diazomethane at room temperature until a persistent pale-yellow color was observed. After evaporation the solvents gave a residue which was purified on a column (120 g) with chloroform/methanol (88:12, v/v) as eluent to give **6** (375 mg, 53%), mp 132-135°C.

$[\alpha]_D^{23}$ −70 (*c* 1.57, MeOH).

MS (FABMS): *m/z* 757 ($M + Na^+$), 735 ($M + H^+$), 717 ($M + H^+ - H_2O$).

MCA-FABMS calc for $C_{36}H_{63}NO_{14}$ + Na: 756.4146, found: 756.42.

Anal calc for $C_{36}H_{63}NO_{14}$: C, 58.92; H, 8.65. Found: C, 58.66; H, 8.40.

Spiroketals of perhydropimaricin-methyl ester **7** *and* **8**

Perhydropimaricin methyl ester **6** (106 mg, 0.14 mmol) in chloroform/methanol (9:1, v/v, 20 mL) at room temperature was treated with camphor sulfonic acid (2 mg, 0.06 equiv) for 2 h. At this time, TLC indicated the formation of two more migrating products and the reaction was quenched by addition of a few drops of pyridine and evaporated *in vacuo*. The residue was purified by column chromatography (100 g) with chloroform/methanol (88:12, v/v) to give first spiroketal **7** (45 mg, 44%) as a colorless glass.

$[\alpha]_D^{23}$ −88 (*c* 1.02, MeOH).

^{1}H NMR (40°C, DMSO-d_6): δ 1.135 (d, 3H, *J* 6.5 Hz, 6′-CH_3), 1.155 (d, 3H, *J* 6.5 Hz, 26-CH_3), 1.84 (s, 3H, NHAc), 3.61 (s, 3H, $COOCH_3$), 3.83 (d, 1H, *J* 6.5 Hz, OH_7), 4.38 (d, 1H, *J* 5.0 Hz, $OH_{2'}$), 4.51 (d, 1H, *J* 5.5 Hz, $OH_{4'}$), 4.92 (d, 1H, *J* 6.5 Hz, OH_{11}), 7.50 (d, 1H, *J* 7.5 Hz, N*H*).

MS (FABMS): *m/z* 739 ($M + H^+$), 717 ($M + H^+$).

MCA-FABMS calc for $C_{36}H_{61}NO_{13}$ + Na: 738.4041, found: 738.40.

Anal calc for $C_{36}H_{61}NO_{13}$: C, 60.40; H, 8.59. Found: C, 60.29; H, 8.75.

The second isomer **8** was then eluted (37 mg, 36%),

$[\alpha]_D^{23}$ −105 (*c* 1.35, MeOH).

^{1}H NMR (40°C, DMSO-d_6): δ 1.15 (d, 3H, *J* 6.5 Hz, 6′-CH_3), 1.155 (d, 3H, *J* 6.5 Hz, 26-CH_3), 1.855 (s, 3H, NHAc), 3.63 (s, 3H, $COOCH_3$), 4.36 (d, 1H, *J* 5.5 Hz, $OH_{2'}$), 4.55 (d, 1H, *J* 5.5 Hz, $OH_{4'}$), 4.70 (d, 1H, *J* 3.0 Hz, OH_7), 4.99 (d, 1H, *J* 7.0 Hz, OH_{11}), 7.50 (d, 1H, *J* 7.5 Hz, NH).

MS (FABMS): *m/z* 739 ($M + Na^+$), 717 ($M + H^+$).

MCA-FABMS calc for $C_{36}H_{61}NO_{13}$ + Na: 738.4041; found: 738.41.

Anal calc for $C_{36}H_{61}NO_{13} \cdot H_2O$: C, 58.92; H, 8.65. Found: C, 58.51; H, 8.57.

Acetylation of the major spiroketal **7**

5,9-Anhydroperhydropimaricin **7** (41 mg, 0.056 mmol) was treated in pyridine (3 mL) with acetic anhydride (1 mL) at room temperature overnight. The reaction mixture was cooled to 0°C and methanol (2 mL) was added dropwise. After 0.5 h, the solvents were removed in vacuo and the residue was submitted to six evaporations from toluene.

The major product was separated from a partially acetylated compound by column chromatography (40 g) using chloroform/methanol (100:2, v/v) to give the tetra-*O*-acetyl derivative **9** (40.5 mg, 79%) as a colorless glass:

$[\alpha]_D^{23}$ −71 (*c* 1.61, $CHCl_3$).

^1H NMR (see tables III and IV); MS (LSIMS): calc for $C_{44}H_{69}NO_{17}$ + Na: 906.4463. Found: 906.4509.

Acetylation of the minor spiroketal **8**

Using the same procedure as described above, the more polar spiroketal **8** (33 mg, 0.045 mmol) gave the tetra-*O*-acetyl derivative **10** (40.5 mg, quantitative) as a colorless glass:

$[\alpha]_D^{23}$ −47 (*c* 0.8, $CHCl_3$).

^1H NMR (see tables III and IV); MS (LSIMS): calc for $C_{44}H_{69}NO_{17}$ + Na: 906.4463. Found: 906.4466.

Acknowledgment

We express our gratitude to Gist-Brocades, The Netherlands, for a generous supply of pimaricin, J Ulrich, *IBS Grenoble*, for mass spectroscopic data and R Green Beau for preparing and correcting this manuscript.

References

1 Current addresses: JM Lancelin, Institut de Biologie Structurale CEA-CNRS, 41 Avenue des Martyrs, 38027 Grenoble Cedex 1, France; JM Beau, Laboratoire de Synthèse de Biomolécules, Institut de Chimie Moléculaire, Université de Paris Sud, 91405 Orsay Cedex, France

2 a) Oroshnik W, Mebane AD, *Prog Chem Org Nat Prod* (1963) 21, 18-79
b) Omura S, Tanaka H, *Macrolide Antibiotics: Chemistry, Biology and Practice*, Omura S Ed, Academic, New York, 1984, pp 351-404

3 Struyk AP, Hoette I, Drost G, Waisvisz JM, Van Eek J, Hoogerheide JC, *Antibiotics Annual, 1957-58*, Welch H, Marti-Ibanez F Eds, Medical Encyclopaedia, New York, 1958

4 Burns J, Holtman DF, *Antibiotics and Chemotherapy*, (1959) 9, 398-405

5 Divekar PV, Bloomer JL, Eastham JF, Holtman DF, Shirley DA, *Antibiotics and Chemotherapy* (1961) 11, 377-380

6 Golding BT, Rickards RW, Meyer WE, Patrick JB, Barber M, *Tetrahedron Lett* (1966) 3551-3557

7 a) Patrick JB, Williams RP, Wolf CF, Weeb JS, *J Am Chem Soc* (1958) 80, 6688-6689
b) Patrick JB, Williams RP, Weeb JS, *J Am Chem Soc* (1958) 80, 6689

8 Ceder O, *Acta Chem Scand* (1964) 18, 126-134 and references cited therein

9 For a review, see Bolard J, *Biochim Biophys Acta* (1986) 864, 257-304

10 Little JR, Blanke TJ, Valeriote F, Medoff G, *Immune Modulation and Control of Neoplasia by Adjuvant Therapy*, Chirigos A Ed, Raven, New York, 1978, pp 381-387

11 Brajtburg J, Kobayashi D, Medoff G, Kobayashi GS, *J Infect Dis* (1982) 146, 138-146

12 Hugues CE, Harris C, Petersen LR, Gerding DN, *Antimicrob Agents Chemother* (1984) 26, 837-840

13 Vertut-Croquin A, Brajtburg J, Medoff G, *Cancer Res* (1986) 46, 6054-6058

14 Henry N, Bolard J, *Biochim Biophys Acta* (1986) 854, 84-92

15 For a review see: Beau JM, *In: Recent Progress in the Chemical Synthesis of Antibiotics*, Lukacs G, Ohno M Eds, Springer, Berlin, 1990, pp 135-182

16 a) Ceder O, Hansson B, Rapp U, *Tetrahedron* (1977) 33, 2703-2714
b) De Bruyn A, Anteünis MJO, Verhegge G, *Bull Soc Chim Belg* (1978) 87, 121-126

17 Pandey RC, Rinehart, Jr KL, *J Antibiot* (1976) 29, 1035-1042

18 Dornberger K, Thrum H, Engelhart G, *Tetrahedron Lett* (1976) 34, 4469-4472

19 The all-*E* geometry of the tetraene chromophore has been deduced from UV spectra of pimaricin, see ref 2a

20 Hempel A, Dauter Z, Bogucka-Lodochowska J, Zielinski J, Borowski E, *Zeitschr Krist* (1977) 146, 315-316

21 Oppong I, Pauls HW, Fraser-Reid B, *J Chem Soc Chem Commun* (1986) 1241-1244

22 Lancelin JM, Beau JM, *J Am Chem Soc* (1990) 112, 4060-4061

23 Duplantier AJ, Masamune S, *J Am Chem Soc* (1990) 112, 7079-7081

24 Lancelin JM, Beau JM, *Tetrahedron Lett* (1989) 30, 4521-4524

25 Rance M, Sørensen OW, Bodenhausen G, Wagner G, Ernst RR, Wüthrich K, *Biochem Biophys Res Commun* (1983) 117, 479-485

26 Bothner-By A, Stephens RL, Lee JM, Jeanloz RW, *J Am Chem Soc* (1984) 106, 811-813

27 Bax A, Davis DG, *J Magn Reson* (1985) 63, 207-213

28 Jeener J, Meier BH, Bachmann P, Ernst RR, *J Chem Phys* (1979) 71, 4546-4553

29 Macura S, Hyang Y, Suter D, Ernst RR, *J Magn Reson* (1981) 43, 259-281

30 Sowiński P, Gariboldi P, Czerwiński A, Borowski E, *J Antibiot* (1989) 52, 1631-1638; *Ibid* 1639-1642

31 Dutcher JD, Walters DR, Wintersteiner O, *J Org Chem* (1963) 87, 121-126

32 Lancelin JM, Paquet F, Beau JM, *Tetrahedron Lett* (1988) 29, 2827-2830

33 Sternhell S, *Q Rev Chem Soc* (1969) 23, 236-270

34 Ernst RR, Bodenhausen G, Wokaun A, *Principles of Nuclear Magnetic Resonance in One and Two Dimensions*, Clarendon, Oxford, 1987

35 Pawlak J, Sowiński P, Borowski E, Gariboldi P, *J Antibiotics* (1993) 43, 1598-1604

36 Sowiński P, Pawlak J, Borowski E, Gariboldi P, *Magn Reson Chem* (1992) 30, 275-279

37 a) Melchinski W, Schaffner CP, Ganis P, *Tetrahedron Lett* (1970) 3873-3876
b) Ganis P, Avitabile G, Melchinski W, Schaffner CP, *J Am Chem Soc* (1971) 93, 4560-4564

38 In reference 24, by error we referred to the configurations at C_4, C_7, and C_9 as *S*, *R*, and *S*, respectively. A subsequent correction was made: *J Am Chem Soc* (1990) 112, 6749

39 The Golding *et al* [6] proposal was based on a further chromic acid degradation yielding glutamic acid (OH at C_5) rather than succinic acid (OH at C_4)

40 Pandey RC, German VF, Nishikawa Y, Rinehart, Jr KL, *J Am Chem Soc* (1971) 93, 3738-3747

41 Rinehart, Jr KL, Tucker WP, Pandey RC, *J Am Chem Soc* (1971) 93, 3747-3751

42 Deslongchamps P, *Stereoelectronic Effects in Organic Chemistry*, Pergamon, Oxford, 1983

43 Marion D, Wüthrich K, *Biochem Biophys Res Commun* (1983) 113, 967-974

44 Cope AC, Burrows EP, Derieg ME, Moon S, Wirth WD, *J Org Chem* (1965) 87, 5452-5460